Surface reactivity of the natural metal (hydr)oxides in weathered tropical soils

Juan C. Mendez [a,b,1], Elise Van Eynde [a,*,1], Tjisse Hiemstra [a], Rob N.J. Comans [a]

[a] *Soil Chemistry and Chemical Soil Quality Group, Wageningen University, 6708 PB Wageningen, the Netherlands*
[b] *Centro de Investigaciones Agronómicas (CIA) and Escuela de Agronomía, Universidad de Costa Rica, 11501-2060 San Pedro de Montes de Oca, Costa Rica*

ARTICLE INFO

ABSTRACT

Assessing the surface reactivity of metal (hydr)oxides in soils is essential for quantifying ion adsorption phenomena that control the availability of nutrients and pollutants. Despite the high natural abundance of Fe and Al (hydr)oxides in intensively weathered environments, the surface reactivity of these pedogenic materials has not been consistently characterized for weathered tropical soils. Here, we used a novel probe-ion methodology combined with state-of-the-art surface complexation modelling (SCM) to derive the reactive surface area (RSA) of the soils, as well as the amount of phosphate (PO_4) that can be potentially desorbed (R-PO_4) from the natural fraction of metal (hydr)oxides and thereby controlling the solid-solution partitioning of PO_4. We applied this methodology to a series of weathered topsoils from the sub-Saharan region. The results showed that nanocrystalline ferrihydrite (Fh) is a better proxy than well-crystallized goethite for describing with SCM the reactivity of the natural metal (hydr)oxides, even though well-crystallized materials dominate the mass fraction of metal (hydr)oxides of these weathered tropical soils. Using Fh as a proxy in the SCM, the RSA ranged from ~2 to 40 m^2 g^{-1} soil. Nanoparticles with a mean diameter of ~1.5–5.0 nm dominate the reactive fraction of metal (hydr)oxides in these tropical topsoils. Our SCM in conjunction with soil extractions indicates that only a fraction of the total PO_4 associated with the metal (hydr)oxides is reversibly adsorbed, whereas the majority of the total PO_4 pool, on average ~64%, is occluded in the crystalline Fe and Al (hydr)oxide fraction. Only this smaller reversibly adsorbed fraction is thus available for participating in sorption reactions that determine the solid-solution partitioning of PO_4. Overall, this research provides new insights into the reactivity of the metal (hydr)oxide fraction in weathered tropical soils and highlights the relevance of these pedogenic materials in determining the speciation and availability of PO_4.

1. Introduction

The bioavailability, mobility, and consequently the risk of deficiencies, toxicities, and leaching of many ions in soils is largely determined by adsorption processes occurring at surfaces of the natural metal (hydr)oxide fraction (Bortoluzzi et al., 2015; Duffner et al., 2014; Regelink et al., 2015). The reactive metal (hydr)oxide materials are particularly relevant for controlling the solid-solution partitioning of oxyanions such as phosphate (PO_4), arsenate (AsO_4), selenite (SeO_3), and others (Hiemstra et al., 2010b; Verbeeck et al., 2017; Zhang et al., 2018). These reactive metal (hydr)oxides are also important for adsorbing soil organic matter (SOM) (Kaiser and Guggenberger, 2000; Wiseman et al., 2005), thereby contributing to the long-term stabilization of organic carbon in soils by forming chemically stable mineral-organic associations (Kleber et al., 2015; Kopittke et al., 2020; Wiesmeier et al., 2019).

The fraction of natural metal (hydr)oxides comprises a series of minerals with variable chemical composition, mineral structure, and crystallinity (Cornell and Schwertmann, 2003; Guo and Barnard, 2013). This different mineral structure may lead to differences in the surface reactivity of these natural metal (hydr)oxides, thereby affecting their adsorption capacity of oxyanions and SOM. The dominant mass fraction and mineral composition of metal (hydr)oxides often vary across different environments (Chen and Thompson, 2018; Perret et al., 2000; van der Zee et al., 2003). For instance, in humid tropics soils are often intensively weathered, which results in a high abundance of Fe and Al

---

(hydr)oxides, mainly present as well-crystallized metal (hydr)oxide material (Basile-Doelsch et al., 2005; Mikutta et al., 2009).

The adsorption of ions to the natural metal (hydr)oxides of soils is a complex process influenced by the amount and surface properties of the mineral phases, the chemistry of the soil solution (e.g. pH, ionic strength, type and concentration of co-existing ions), and the competitive or cooperative interaction of negatively charged SOM (Weng et al., 2011). In this context, surface complexation models (SCMs) are envisioned as promising tools for analyzing how these multiple factors interact and affect the overall ion adsorption behavior of soil systems (Di Bonito et al., 2018; Goldberg, 2014; Groenenberg and Lofts, 2014). These SCMs use a set of thermodynamic relationships for describing the chemical and electrostatic equilibrium interactions between ions and the reactive surface groups of metal (hydr)oxides. A successful application of SCMs in soils requires a consistent characterization of the surface reactivity of the metal (hydr)oxide fraction. However, despite the naturally high content of Fe and Al (hydr)oxides in weathered soils from the tropics, a consistent characterization of the surface reactivity of the natural metal (hydr)oxides is not available for this type of soils.

The reactive surface area of soils (RSA, expressed in $m^2 g^{-1}$ soil) due to the presence of the pedogenic metal (hydr)oxides is a key feature determining the capacity of soils for adsorbing oxyanions and for interacting with SOM (Eusterhues et al., 2005; Mayer, 1994; Mendez et al., 2020). In this paper, the term RSA comprises all the reactive surfaces of naturally occuring metal (hydr)oxides that determine the equilibrium soil–solution partitioning of a chosen probe ion (i.e. phosphate), and whose reactivity is represented by a reference oxide material with a well-characterized surface reactivity. Thus, an "*effective*" reactive surface area rather than a total or an absolute surface area is determined.

A consistent assessment of the RSA of soils is not trivial, and multiple challenges are faced when using traditional analytical approaches. Gas adsorption analysis using for instance N_2 or Ar as probe molecules, and subsequent interpretation with the Brunauer-Emmett-Teller (BET) equation (Brunauer et al., 1938), is a classical approach commonly used for assessing the surface area of synthetic oxides. It has also been applied to soils (Coward et al., 2018; Eisazadeh et al., 2013; Fontes and Weed, 1996). However, this approach has several disadvantages (Heister, 2014). Drying and outgassing the samples prior to the gas adsorption analysis provoke irreversible aggregation of colloidal nanoparticles, which leads to an underestimation of the RSA (Dzombak and Morel, 1990; Mendez and Hiemstra, 2020). Moreover, part of the mineral surface area is covered by adsorbed SOM and might not be accessible for the probe gas molecules (Mödl et al., 2007). Attempts to remove the SOM before the gas adsorption analysis, for instance by oxidizing the SOM (Coward et al., 2018), may change the physical-chemical properties of the mineral surfaces, also affecting the measured RSA (Hiemstra et al., 2010a).

An alternative to gas adsorption is the use of ethylene glycol monoethyl ether (EGME) as a probe molecule for assessing the RSA of soils (Cihacek and Bremner, 1979), but this approach provides mainly an estimation of the surface area of aluminosilicate clay minerals (Kennedy et al., 2002). Humic acids adsorption has been proposed for assessing the surface area contribution of kaolinite and goethite in the fine fraction (<45 μm) of river sediments, but this method only provides an estimation of the relative surface area of the components in binary mineral systems (e.g. kaolinite-goethite), rather than offering the overall RSA for the whole metal (hydr)oxide fraction (Dong and Wan, 2014).

Another alternative approach to estimating the RSA of soils is based on measuring the amount of Fe and Al with selective dissolution extractions of soils, such as for instance acid ammonium oxalate and dithionite citrate extractions. Using these data, the RSA of the soil is then calculated by applying a set of "standard" values for the specific surface area (SSA) and molar mass of the crystalline and nanocrystalline metal (hydr)oxide fraction (Dijkstra et al., 2009; Groenenberg et al., 2017; Tiberg et al., 2018; Weng et al., 2001). However, the SSA of metal (hydr) oxides greatly varies across different soil samples (Hiemstra et al.,

2010a; Mendez et al., 2020). Moreover, the molar mass, mass density, and surface curvature of metal (hydr)oxide nanoparticles are size-dependent (Mendez and Hiemstra, 2020) and the use of single values will therefore introduce inconsistencies in the calculation of RSA.

Recently, it has been proposed to calculate the RSA of soils using PO_4 as a probe-ion (Hiemstra et al., 2010a). This oxyanion is natively present in all soils and has a high binding affinity for Fe and Al (hydr)oxides. In this methodology, the competitive adsorption interaction between CO_3 and PO_4 is measured in a 0.5 M $NaHCO_3$ solution of pH = 8.5. Simultaneously, this method allows estimating by SCM the amount of PO_4 that is potentially desorbable from the metal (hydr)oxide surfaces (R-PO_4). In the probe-ion approach, a desorption curve is established by applying a range of solution-to-solid ratios (SSR) in the soil extractions. The results are then interpreted with the charge-distribution (CD) model (Hiemstra and Van Riemsdijk, 1996), using a chosen metal (hydr)oxide material as reference for which the competitive adsorption isotherms of PO_4 have been well parameterized in synthetic systems in the presence of CO_3 ions. Recently, we have shown, for a set of agricultural topsoils from a temperate climate, that the reactivity of the natural metal (hydr)oxides is better described when nanocrystalline ferrihydrite (Fh), rather than well-crystallized goethite, is used as a reference oxide material in the CD model (Mendez et al., 2020).

In highly weathered soils from the humid tropics, crystalline Fe and Al (hydr)oxides (e.g. goethite, hematite, gibbsite) generally dominate the fraction of pedogenic metal (hydr)oxides (Cornell and Schwertmann, 2003; Kleber et al., 2007; Xu et al., 2016), while the contribution of (hydr)oxide nanoparticles (i.e. Fh-like materials) may be relatively small on a mass basis. Nevertheless, it is still possible that these nanosized materials greatly contribute to the overall reactivity of soils, even at low concentrations, because the SSA of these nanoparticles is substantially higher than the SSA of the crystalline metal (hydr)oxides. Therefore, the question arises of how well the overall behavior of the metal (hydr)oxide fractions of weathered tropical soils can be represented using synthetic materials as proxies. One of the objectives of the present study is to answer this question.

The probe-ion method implemented in this study uses phosphorus (P) that is naturally present in soils to quantify the overall surface reactivity of the metal (hydr)oxide fraction. In soils, P can be categorized in pools with different chemical behavior and bioavailability. Generally, these different P fractions are operationally defined with selective extraction methods (Weihrauch and Opp, 2018). The separation between organic and inorganic P pools is one of the most common distinctions made in the literature. For the inorganic P pool, different PO_4 fractions with different lability can be also distinguished, i.e. soluble phosphate, reversibly adsorbed phosphate, and phosphate that is occluded within metal (hydr)oxide particles. The relative contribution of the different P pools in soils might change according to the soil weathering stage and the composition of the metal (hydr)oxide fraction (Weihrauch and Opp, 2018; Yang and Post, 2011), and therefore, it may vary significantly for intensively weathered soils from the tropics, compared to soils from temperate climates.

In the present study, we will discuss the results of the probe-ion method applied to a series of weathered topsoil samples from sub-Saharan African countries. The results will be interpreted with the CD model using either Fh or goethite as the reference metal (hydr)oxide. The choice of these materials as proxies for the reactive metal (hydr) oxide fraction in soils has been motivated by the existence of internally consistent databases with intrinsic adsorption parameters (Mendez and Hiemstra, 2019; Rahnemaie et al., 2007) and detailed knowledge of the surface structure of these model Fe (hydr)oxides (Hiemstra and Van Riemsdijk, 1996; Hiemstra and Zhao, 2016). In addition, Fh and goethite have a contrasting specific surface area (SSA, expressed in $m^2 g^{-1}$ oxide material) and mineral crystallinity, as well as a distinct CO_3-PO_4 surface interaction (Mendez et al., 2020; Mendez and Hiemstra, 2019; Rahnemaie et al., 2007). This will allow us to evaluate which type of model material represents best the overall behavior of the natural metal (hydr)

oxide fraction in these soils.

The RSA values obtained with the probe-ion method, combined with experimental data of selective dissolution extractions, will be used to assess the properties of the reactive metal (hydr)oxides of these topsoils. To do so, a novel approach is applied that estimates, in a self-consistent manner, the size-dependent values of specific surface area (SSA), molar mass (M_{nano}), and mass density (ρ_{nano}) of the metal (hydr)oxide nanoparticles in soils (Mendez et al., 2020). Regarding the different P pools, we will assess the potential contribution of occluded PO_4 to the total pool of PO_4 associated with the metal (hydr)oxide minerals. For this purpose, we will measure the amount of PO_4 in the dithionite-citrate extracts and compare the results to the amount of reversibly bound PO_4 (R-PO_4). Additionally, we will analyze the relative contribution of the organic P and the inorganic PO_4 pools in the ammonium oxalate (AO) extracts and will compare the results with those of the series of topsoils from a temperate climate that has been characterized previously with regard to these properties (Mendez et al., 2020).

2. Materials and methods

2.1. General soil characteristics

From a larger set of soil samples from sub-Saharan African countries, 18 samples were selected based on their differences in pH, soil organic carbon (SOC) content, acid ammonium oxalate (AO) extractable PO_4, and Fe and Al-(hydr)oxides content. The soils originate from Burundi (samples 1–15) and Kenya (samples 16–18). Several general characteristics of the selected soil samples are shown in Table 1. According to the Soil Grids system (Hengl et al., 2016), based on the World Reference Base (WRB) soil classification system, the majority of the soils are classified as Acrisols and Ferralsols, which are typically highly weathered soils from the humid tropics, generally known for their inherent low soil fertility and high P adsorption capacity. Based on this classification and in the absence of a specific mineralogical analysis, the clay fraction of these weathered tropical soils is likely dominated by kaolinitic materials with relatively low surface area and by pedogenic Fe and Al (hydr)oxides.

In addition, we will compare the results presented here for weathered tropical soils with those obtained previously for a set of agricultural

Table 1
Chemical characteristics and modelling results of the soil samples selected for the present study.

Soil	OC	<2 μm	AO-Fe [a]	AO-Al [a]	AO-P_{tot} [a]	AO-PO_4 [a]	DC-Fe [b]	DC-Al [b]	DC-P_{tot} [b]	DC-PO_4 [b]	CaCl₂ pH [c]	CaCl₂ PO_4 [c]	R-PO_4 Gt [d]	R-PO_4 Fh [e]	RSA Gt [d]	RSA Fh [e]
	%	%	mmol kg⁻¹									μM	mmol kg⁻¹		m² g⁻¹	
1	1.4	33	20.1	42.3	4.4	2.4	332.1	98.3	11.3	7.8	4.4	0.39	3.94 ± 0.10	2.09 ± 0.30	3.89 ± 0.08	8.24 ± 0.70
2	1.5	7	20.8	50.7	4.7	2.5	289.9	97.2	9.9	6.7	4.1	0.40	3.80 ± 0.07	1.94 ± 0.07	3.73 ± 0.07	6.62 ± 0.39
3	5	7	156.2	314.3	11.4	4.3	458.7	328.7	10.6	4.3	4.3	0.09	9.25 ± 0.125	2.96 ± 0.08	12.29 ± 0.07	15.50 ± 0.05
4	2	71	48.9	132.8	2.5	1.5	996.1	186.8	8.1	5.2	4.1	0.05	2.45 ± 0.09	1.26 ± 0.15	4.80 ± 0.19	23.04 ± 2.83
5	2.8	10	70.7	168.2	7.5	3.2	492.1	244.7	11.9	6.1	4.4	0.07	6.25 ± 0.07	2.71 ± 0.09	8.25 ± 0.12	16.88 ± 0.58
6	2.4	12	41.2	138.3	7.5	5.2	510.1	202.5	11.0	7.9	5.0	0.25	15.89 ± 0.13	7.22 ± 0.25	16.36 ± 0.07	24.74 ± 0.26
7	1.9	12	27.8	76.3	3.1	1.3	373.7	180.7	9.7	5.6	5.1	0.09	2.34 ± 0.02	1.38 ± 0.04	3.15 ± 0.02	12.54 ± 0.44
8	1.4	7	20.7	51.3	2.6	1.7	310.1	134.9	7.4	5.1	4.5	0.19	3.94 ± 0.14	2.01 ± 0.12	4.57 ± 0.10	11.24 ± 0.51
9	2.1	2	77.7	94.5	7.6	2.9	342.2	215.0	15.4	9.5	4.5	0.10	5.94 ± 0.064	2.98 ± 0.08	6.29 ± 0.06	12.09 ± 0.14
10	2.2	17	57.6	147.5	3.9	1.7	646.7	253.0	8.7	4.8	4.2	0.04	3.03 ± 0.08	1.59 ± 0.03	5.77 ± 0.18	27.83 ± 0.08
11	2.2	4	59.5	152.1	4.0	1.5	615.9	245.1	8.7	4.5	4.3	0.04	3.20 ± 0.07	1.54 ± 0.03	7.06 ± 0.13	39.13 ± 0.47
12	1.4	4	37.3	63.3	3.4	1.4	327.6	139.5	8.0	4.7	4.2	0.06	2.57 ± 0.02	1.15 ± 0.05	3.58 ± 0.02	11.07 ± 0.24
13	1.2	5	37.8	63.6	3.3	1.6	327.8	141.1	8.4	4.8	4.1	0.08	2.46 ± 0.02	1.32 ± 0.03	3.36 ± 0.02	12.59 ± 0.37
14	1.5	7	41.5	70.9	4.1	2.1	325.2	141.3	8.3	4.9	4.2	0.08	2.72 ± 0.04	1.54 ± 0.03	3.48 ± 0.03	12.99 ± 0.18
15	3.2	8	65.7	135.9	4.0	1.5	730.3	171.7	9.1	4.8	4.9	0.09	2.53 ± 0.05	1.20 ± 0.07	3.88 ± 0.08	10.34 ± 0.17
16	0.9	7	56.9	56.1	22.3	16.9	289.5	90.7	32.5	–	5.3	2.23	25.85 ± 0.18	14.25 ± 0.22	15.14 ± 0.05	9.69 ± 0.03
17	0.3	20	7.8	24.1	2.1	2.2	67.0	39.4	3.2	–	6.8	1.61	2.39 ± 0.05	1.57 ± 0.04	1.43 ± 0.05	1.70 ± 0.06
18	0.6	53	32.9	40.4	1.7	1.6	634.9	58.2	6.1	–	6.3	0.16	1.51 ± 0.13	0.92 ± 0.05	1.51 ± 0.14	3.47 ± 0.14

[a] Measured with acid ammonium oxalate extraction (pH = 3) (ISO, 2012a).
[b] Measured with dithionite-citrate extraction (ISO, 2012b).
[c] Measured in 0.01 M CaCl₂ (solution-to-solid ratio SSR = 10 L kg⁻¹, time = 2 h) (Houba et al., 2000).
[d] Pool of reversely bound PO_4 (R-PO_4) and reactive surface area (RSA) derived with the results of the probe-ion method, using goethite as reference oxide material in the CD modelling.
[e] Pool of reversely bound PO_4 (R-PO_4) and reactive surface area (RSA) derived with the results of the probe-ion method, using ferrihydrite as reference oxide material in the CD modelling.

soils samples from a temperate environment with the same approach as applied in this study. The chemical characteristics of these soil samples are given in Hiemstra et al. (2010b) and Mendez et al. (2020).

2.2. Chemical analyses for samples characterization

Total SOC content of the soils was analyzed using a wet oxidation method according to the Kurmies procedure and measured with a spectrophotometer (Nelson and Sommers, 1996). The clay content was measured by laser-diffraction after pre-treatment with H_2O_2 and HCl while standing in a warm water bath. The volume percentage of the particle fraction smaller than 2 µm was re-calculated to the mass percentage of clay using a particle density of 2.6 g cm^{-3} and a bulk density of 1.3 g cm^{-3}. The pH was measured with a glass electrode in a 0.01 M $CaCl_2$ soil extract, at an SSR of 10 L kg^{-1} (Houba et al., 2000).

The nanocrystalline fractions of Fe and Al (hydr)oxides of the soils were estimated using an acid ammonium oxalate (AO) extraction (ISO, 2012a). Dried soil samples were extracted with a solution (pH 3.0 ± 0.1) containing 0.1 M di-ammonium oxalate and 0.1 M oxalic acid at an SSR of 20 L kg^{-1}. Samples were equilibrated in the dark at a constant temperature of 20 °C and continuously shaken using an end-over-end shaker. After equilibration for 4 h, samples were centrifuged at 2100g for 30 min and an aliquot of the supernatant was filtered over a 0.45 µm membrane filter. The filtrates were measured for Al (AO-Al), Fe (AO-Fe), and total P (AO-P_{tot}) using an ICP-OES (Thermo Scientific iCAP6500). In a separate batch of AO soil extracts, the concentration of orthophosphate (AO-PO_4) was analyzed using a segmented flow analyzer (SFA), applying the colorimetric molybdenum-blue method (Murphy and Riley, 1962). For the AO-PO_4 analysis, the samples were diluted 100 times with demineralized water to eliminate the interference of oxalate in the colorimetric reaction (Cui and Weng, 2013; Hass et al., 2011). Preliminary tests showed no differences in the PO_4 concentration measured with either 10- or 100-times dilution of the AO soil extracts. We applied the ISO protocol for AO extractions which prescribes an extraction time of 4 h (ISO, 2012a), while this extraction method had been originally established using an extraction time of 2 h (Schwertmann, 1964). We assessed the effect of using either 4 or 2 h as extraction time on the measured concentrations of AO extractable P_{tot}, PO_4, Al, and Fe. For inorganic PO_4 measurements, the concentration increased on average only by ~10% when increasing the equilibration time from 2 to 4 hrs, while this increment was larger for P_{tot} (22%), Al_{AO} (27%), and Fe_{AO} (40%).

Dithionite-citrate (DC) extractions were performed to assess the crystalline metal (hydr)oxide fraction. The DC extractions were done using the ISO protocol (ISO, 2012b). Briefly, dried soil samples were extracted with a mixture of 0.3 M sodium acetate, 0.2 M trisodium citrate, and 0.3 M sodium dithionite, adjusted to pH 4.8 with sodium acetate, at an SSR of 20 L kg^{-1}. Samples were equilibrated for 3.5 h in a water bath at 60 °C. After equilibration, samples were centrifuged at 3000g for 30 min and an aliquot of the supernatant was filtered over a 0.45 µm membrane filter. The filtrates were subsequently analyzed for Fe (DC-Fe), Al (DC-Al), and total P (DC-P_{tot}) by ICP-OES, and for ortho-PO_4 (DC-PO_4) by SFA using the colorimetric molybdenum-blue method (Murphy and Riley, 1962). For the samples 16–18 of the sub-Saharan series, the DC-PO_4 pool was not analyzed. Similar to the AO extracts, the DC extracts were diluted (100 times) with demineralized water prior to the colorimetric analyses of PO_4. The fraction of crystalline Fe and Al (hydr)oxides was estimated as the difference between the DC- and AO-extractable amounts of Fe and Al.

2.3. Equilibrium $NaHCO_3$ extractions

PO_4 desorption data were collected applying the probe-ion method proposed by Hiemstra et al. (2010a). In this method, soil extractions with a 0.5 M $NaHCO_3$ solution of pH 8.5 are performed to promote PO_4 desorption from the soil mineral surfaces (Barrow and Shaw, 1976).

First, a fresh 0.5 M $NaHCO_3$ solution was prepared by dissolving 21.2 g of $NaHCO_3$ in 0.5 L of demineralized water. The pH of the $NaHCO_3$ solution was then adjusted to 8.5 using a 2 M NaOH solution. Dried soil samples were extracted with the 0.5 M $NaHCO_3$ solution at six different SSR of 10, 20, 50, 80, 100, and 200 L kg^{-1}. For the three lowest SSRs, soils were extracted with 20 mL of the $NaHCO_3$ solution in 50 mL polyethene tubes, whereas, for the three highest SSRs, soils were extracted with 90 mL of $NaHCO_3$ in polyethene 225 mL bottles. These conditions led to a constant gas-to-solution volume ratio of 1.5 L L^{-1} among all SSR.

In soils, the presence of SOM may affect the $PO_4 - CO_3$ interaction due to competition with PO_4 for the binding sites at the soil surfaces. To suppress this possible effect during the $NaHCO_3$ extractions and facilitate the measurement of PO_4, an excess of powdered activated carbon (AC) was added (0.40 g g^{-1} soil) to the soil suspensions (see Hiemstra et al., (2010b) for further explanation). Because the AC might contain small amounts of PO_4, the AC was pre-cleaned with an AO-solution (Koopmans et al., 2020). An additional rinsing step with 0.5 M $NaHCO_3$ was included before drying the AC at 40 °C for 3 days. For each extraction batch, blank samples were included containing only AC and the $NaHCO_3$ solution. The P-PO_4 concentration in these blank samples ranged from 0.01 to 0.05 mg L^{-1}, which was relatively low compared to the PO_4 concentration measured in the supernatants of the soil samples (0.13–12.45 mg L^{-1}P-PO_4).

In a pre-experiment, we evaluated the kinetics of PO_4 desorption in the $NaHCO_3$ solution using three soil samples from the sub-Saharan series at two different SSR (10 and 100 L kg^{-1}). The samples were shaken for 24, 168, 336, 504, and 672 h in an end-over-end shaker at 30 cycles per min. Based on the kinetic experiment, a final equilibration time of 504 h (21 days) was used for the main experiment. After equilibration, the pH was measured with a glass electrode and the samples were centrifuged at 3000g for 10 min and filtered over 0.45 µm membrane filters. Before measuring the PO_4 concentration using the colorimetric molybdenum-blue method (Murphy and Riley, 1962), the filtrate was diluted (3 times) with a 0.3 M HCl solution to adjust the pH value to pH ~ 2, and the excess CO_2 was removed from the filtrate by degassing these solutions in an ultrasonic bath for ~10 min.

2.4. Assessment of reactive surface area and reactive phosphate pool

The charge distribution (CD) model (Hiemstra and Van Riemsdijk, 1996) was used to derive the reactive surface area (RSA expressed in m^2 g^{-1} soil) of each soil sample. In this approach, the model-calculated PO_4 concentrations were fitted to the experimental concentrations measured in the 0.5 M $NaHCO_3$ extraction solution at different SSRs. In addition, the amount of reactive PO_4 that can potentially be desorbed from the mineral soil surfaces (R-PO_4 expressed in mol kg^{-1} soil) is simultaneously found by modelling. The underlying calculations to derive RSA and R-PO_4 with the CD model have been explained in detail by Hiemstra et al. (2010b) and Mendez et al. (2020), and are also provided in Appendix 1 of the Supporting Information.

The RSA and R-PO_4 of the soils were calculated by using in the CD model either ferrihydrite (Fh) or goethite as a proxy for the fraction of reactive natural metal (hydr)oxides. In the modelling, the surface interaction between PO_4 and CO_3 is described using an internally consistent thermodynamic database derived previously in model systems with freshly prepared Fh nanoparticles (Mendez and Hiemstra, 2019) and well-crystallized goethite (Rahnemaie et al., 2007). Both materials have quite different CO_3-PO_4 interactions. The CD model is combined with state-of-the-art multi-site ion complexation (MUSIC) models for the specific model (hydr)oxide considered (Hiemstra and Van Riemsdijk, 1996; Hiemstra and Zhao, 2016). The model calculations were done using the ECOSAT program (version 4.9) (Keizer and Van Riemsdijk, 1995) in combination with the FIT program (version 2.581) (Kinniburgh, 1993) for optimization of the RSA and R-PO_4 values.

2.5. Data analysis

To identify which reference material, either Fh or goethite, is a better proxy for the natural metal (hydr)oxide fraction in our set of soils, the amount of PO_4 extracted by the selective dissolution extractions (i.e. AO and DC) was compared to the $R-PO_4$ pool obtained by modelling the PO_4 desorption curves measured in 0.5 M $NaHCO_3$. To establish relations between the RSA and the metal (hydr)oxide content and between the P pools and various soil properties, linear and non-linear regression analysis was done using the data analysis tool in Excel. For each of these relations, the regression equation with the coefficient estimates was given, together with the coefficient of determination (R^2) to show the variance explained by the regression model.

3. Results and discussion

3.1. Phosphate desorption in 0.5 M $NaHCO_3$ extractions

In Fig. 1, the equilibrium PO_4 concentration in the 0.5 M $NaHCO_3$ soil extracts as a function of the SSR is given for six selected samples. For all SSRs, the measured PO_4 concentrations were considerably higher than our detection limit for measuring PO_4 colorimetrically in the 0.5 M $NaHCO_3$ soil extracts (dotted horizontal line in Fig. 1). From an analytical and a practical perspective, this observation is important because the probe-ion method was first developed and tested for agricultural topsoils from temperate climates, which generally have high concentrations of soluble PO_4 (Hiemstra et al., 2010a).

As expected, the highest PO_4 concentrations in the soil extracts are found at the lowest SSR. When the SSR increases (i.e. when the soil sample is further diluted with $NaHCO_3$ solution), the equilibrium PO_4 concentrations decrease but less than expected from the imposed
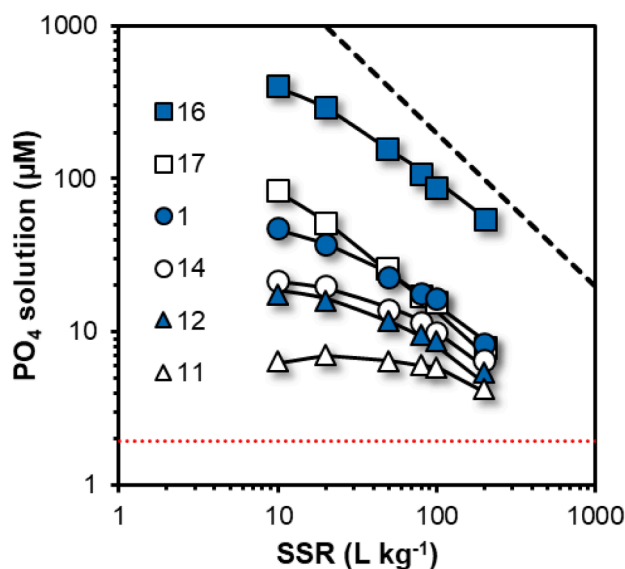
Fig. 1. Phosphate (PO_4) concentration in the 0.5 M $NaHCO_3$ solution at a pH value near 8.5 as a function of the solution-to-solid ratio (SSR) shown here for six selected soil samples which are referred to by the sample numbers used in Table 1. The full lines connect the CD model calculations for each SSR, using ferrihydrite as reference metal (hydr)oxide material. In the modelling, both the RSA and $R-PO_4$ are defined as adjustable parameters. The model parameters used to describe the competitive interaction of CO_3-PO_4 were taken from Mendez and Hiemstra (2019). The dashed diagonal line represents a theoretical linear dilution curve, i.e. a 10 times decrease in SSR results in a 10 times lower PO_4 concentration in solution. The experimental data shows a lower slope than the linear dilution curve, which is due to the release of additional PO_4 from the soil surfaces (i.e. PO_4 buffering) when the SSR increases. The red dotted horizontal line represents the lowest measurable concentration of PO_4 in the 0.5 M $NaHCO_3$ solution with our analytical procedure.

dilution factor, because additional PO_4 is released from the soil surfaces. The PO_4 buffering of the soil leads to the non-linearity of the dilution curves. In Fig. 1, the slope of the PO_4 dilution curves is therefore related to the PO_4 buffer capacity of the soil, which is in turn determined by the reactive surface area of the soil (Hiemstra et al., 2010a). Soils with less steep dilution curves are expected to have a higher RSA. If soil does not release any additional PO_4 upon soil sample dilution with $NaHCO_3$, the experimental PO_4 concentration will decrease linearly with the SSR (dashed line in Fig. 1). As inferred from Fig. 1, the PO_4 buffer capacity (slope of the dilution curve) and consequently the RSA, greatly differs among the selected soil samples.

3.2. Phosphate fractions associated with the metal (hydr)oxides

3.2.1. Reactive pool of adsorbed phosphate

The pool of reactive PO_4 potentially available for desorption from the soil surfaces ($R-PO_4$) can be revealed by interpreting the results from the probe-ion method with the CD model. This $R-PO_4$ pool controls the calculated solid-solution partitioning of PO_4 in the 0.5 M $NaHCO_3$ soil extractions at different SSRs. The size of the calculated $R-PO_4$ pool depends on the properties of the metal (hydr)oxide chosen as reference, in our study either goethite or Fh (Mendez et al., 2020; Mendez and Hiemstra, 2019). In this section, we compare the modelled $R-PO_4$ values with the amount of inorganic PO_4 that is measured in the soil extracts of a selective dissolution methodology. Specifically, our benchmark will be finding agreement between the experimental PO_4 pool measured by the AO extraction and the modelled $R-PO_4$ pool. AO extractions are often applied to selectively dissolve and quantify the nanocrystalline fraction of Fe and Al (hydr)oxides in soils (Borggaard, 1992; Schwertmann, 1973; Schwertmann et al., 1982). Long-term experiments have shown that nearly all the colorimetrically measured P (i.e. ortho-PO_4) that is extracted with AO is potentially desorbable when the soil is exposed to an "infinite" sink condition for P (Lookman et al., 1995). In line with these results, others have found that a large fraction of total P measured in AO extracts was desorbable in a long-term P-mining pot experiment (Koopmans et al., 2004). Additionally, on average, ~65% of the AO-PO_4 pool was desorbed from our weathered tropical soils in the extractions with 0.5 M $NaHCO_3$ (pH = 8.5) at the highest SSR of 200 L kg^{-1}. For a series of P-rich soil from a temperate climate (Mendez et al., 2020), this average value was even larger; ~80% of the AO-PO_4 was desorbed in the 0.5 M $NaHCO_3$ soil extractions at a SSR of 300 L kg^{-1}. These findings show that a large fraction of the AO-PO_4 can be desorbed from the soil mineral surfaces in mild $NaHCO_3$ extraction, even though "infinite" sink conditions were not present.

In the AO soil extracts, the total pool of released P (AO-P_{tot}) can also be conveniently analyzed by ICP-OES, simultaneously with the analysis of Fe and Al. In the original probe-ion approach developed by Hiemstra et al.(2010a), the calculated $R-PO_4$ was compared with the AO-P_{tot} pool measured by ICP-OES, rather than with the fraction of ortho-PO_4 (AO-PO_4) measured using the colorimetric molybdenum-blue methodology (Hass et al., 2011; Murphy and Riley, 1962; Worsfold et al., 2016). However, the AO-P_{tot} pool may also include other P species than ortho-PO_4, especially organic P (P_{org}) (Wolf and Baker, 1990), whereas the probe-ion method is based on the measurement of the equilibrium concentration of ortho-PO_4 in the 0.5 M $NaHCO_3$ extracts. For instance, inositol phosphates, the most abundant organic P form in soils, can be effectively extracted with AO solutions (Jørgensen et al., 2015). Therefore, we have used in the present study AO-extractable PO_4 rather than AO-P_{tot}, as a validation criterion in our evaluation of the $R-PO_4$ values obtained by CD modelling.

Fig. 2a shows the modelled $R-PO_4$ values using Fh as reference metal (hydr)oxide in relation to the experimental AO-PO_4 pool. In general, a good agreement (1:1 line) is observed between both model and experimental PO_4 pools, while this is not the case when goethite is used as reference metal (hydr)oxide in the CD modelling. In the latter case, as is also shown in Fig. 2a, the $R-PO_4$ values predicted by the model are ~2
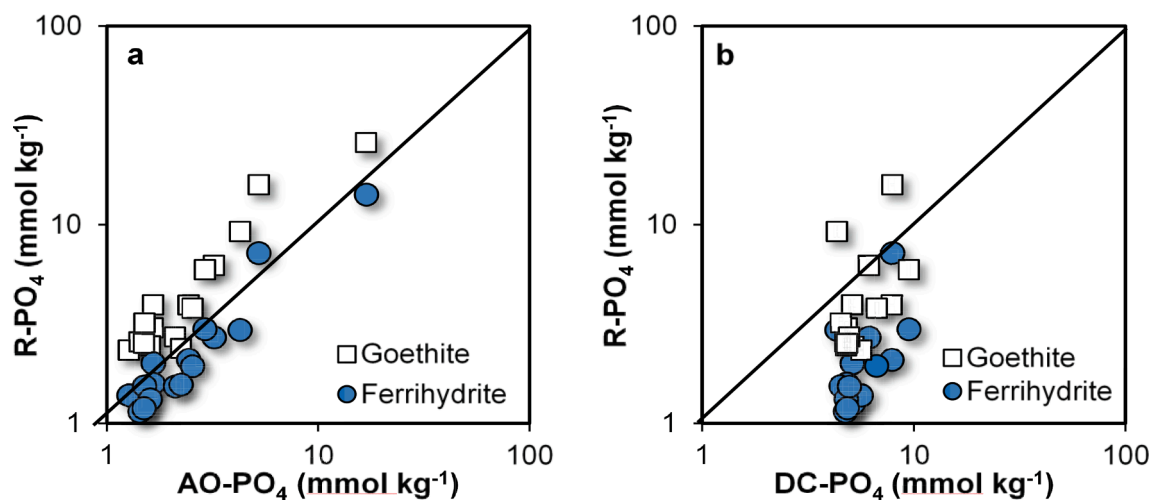
Fig. 2. Comparison between the amount of reactive PO_4 that is potentially desorbed from the soil surfaces (R-PO_4), calculated with the CD model using either goethite or Fh as reference metal (hydr)oxide, and experimental measurements of PO_4 in the (a) ammonium oxalate (AO) extracts or (b) in the dithionite-citrate (DC) extracts of the series of sub-Saharan African soil samples. Both x-and y- axes are shown based on the $\log_{10}$ scale. In panel b, samples 16–18 are not included because DC-PO_4 data are not available for these samples. The solid line in both figures represents the 1:1 line.

times higher than the experimental AO-PO_4 pool. Therefore, based on the AO-PO_4 data as the validation criterion, we conclude that Fh is a better proxy for the reactive fraction of Fe and Al (hydr)oxides of these weathered tropical topsoils from sub-Saharan Africa. This observation is remarkable considering that, on a mass basis, well-crystallized materials (i.e. goethite-like materials) are clearly the dominant fraction of metal (hydr)oxides in our set of tropical soil samples (Table 1).

3.2.2. Phosphate occluded in the crystalline metal (hydr)oxides

In addition to the soil extractions with AO solution, soils can also be extracted with a dithionite-citrate (DC) solution to assess the total content of Fe and Al (hydr)oxides, comprising both the fraction of nanocrystalline and well-crystallized metal (hydr)oxides (Aguilera and Jackson, 1953; Mehra and Jackson, 1958). Because our tropical topsoils have a relatively high content of crystalline metal (hydr)oxides (Table 1), we have also measured the pool of inorganic PO_4 extracted with DC (DC-PO_4) for a subset of soils.

As shown in Fig. 2b, the DC-PO_4 pool is considerably larger than the corresponding R-PO_4 values calculated by CD modelling using Fh as a proxy. Using goethite as reference material also did not provide a good relationship between DC-PO_4 and R-PO_4 (Fig. 2b). In both cases, the lack of agreement between experimental and modelled values suggests that an important fraction of DC-PO_4 is not desorbable and does not play a significant role in the solid-solution partitioning of PO_4 in the soil extractions with 0.5 M $NaHCO_3$ solution.

The amount of PO_4 that is associated with the crystalline metal (hydr)oxide fraction ($PO_{4,crys}$) can be defined operationally as the difference between DC and AO extractable PO_4. This $PO_{4,crys}$ pool is not part of the PO_4 equilibration process. Likely, it is bound internally as occluded PO_4, similarly as found in synthetic systems when Fh crystallizes to hematite and goethite in the presence of PO_4 (Gálvez et al., 1999). Also in those synthetic systems, the fraction of occluded PO_4 was not desorbable from the mineral surfaces in repeated extraction cycles with an alkaline solution. In our samples, with soil 3 as an exception, the
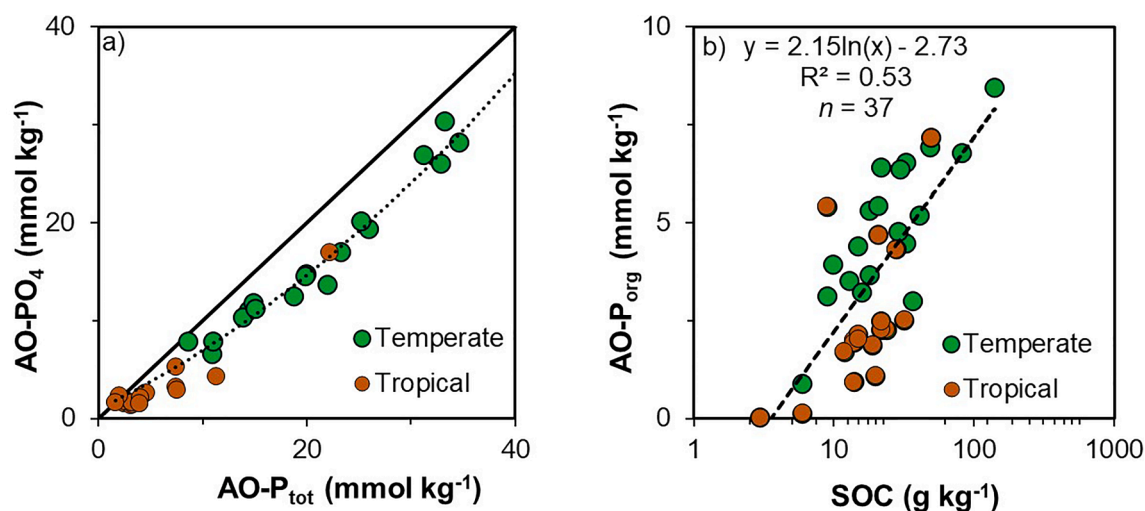

Fig. 3. Panel a: Relationship between the total P and the amount of ortho PO_4 that is extracted from temperate and tropical soils with an acid ammonium oxalate (AO) solution (pH = 3). The diagonal full line represents the 1:1 line, whereas the curved dotted line has been added to guide the eye. Panel b: Relationship between the amount of soil organic carbon (SOC) and the P_{org} pool. The latter is operationally defined as the difference between AO-P_{tot} and AO-PO_4. The dashed line represents the logarithmic regression curve. The red symbols are for the samples collected from agricultural tropical topsoils from sub-Saharan countries. The green symbols are for a series of agricultural topsoils from a temperate region analyzed previously (Hiemstra et al., 2010a; Mendez et al., 2020) and this information is shown here for comparison.

occluded pool of PO_4 is $64 \pm 11\%$ of total DC-extractable PO_4.

3.2.3. Organic phosphorus bound to the reactive metal (hydr)oxides

In the AO-extracts, the total amount of phosphorus (P_{tot}) is systematically higher than the amount of ortho-PO_4. This is shown in Fig. 3a for the present set of weathered tropical soils, as well as for soils from a temperate climate analyzed in our previous study (Mendez et al., 2020). These results highlight the importance of distinguishing analytically between the ortho-PO_4 fraction and the total P pool measured in the AO extracts when using the results of this extraction methodology as a proxy for the pool of reactive PO_4 in soils. In other SCM studies (Verbeeck et al., 2017; Warrinnier et al., 2019), the use of AO-P_{tot} as a proxy for R-PO_4 has led with modelling to overestimations of the PO_4 concentration in soil leachates (Warrinnier et al., 2019) and soil extraction solutions (Verbeeck et al., 2017). Based on those results, the use of isotopically exchangeable PO_4 (*E*-value) has been proposed as a proxy for R-PO_4 in SCM. However, the contribution of organic P species to the AO-P_{tot} was not explicitly considered, whereas it can significantly contribute to the total pool of P measured in AO extractions, as we have shown here. In addition, measurement of the isotopically exchangeable PO_4 pool may be strongly influenced by the kinetics of P exchange and the predefined evaluation time (Frossard and Sinaj, 1997).

When defining the amount of organic P in the AO extracts (AO-P_{org}) as the difference between AO-P_{tot} minus AO-PO_4, a positive relationship is found between AO-P_{org} and the total SOC content of the soil samples (Fig. 3b). A similar type of relationship has also been found for the agricultural topsoils from a temperate climate analyzed in our previous study (Mendez et al., 2020). Fig. 3b shows the relationship between AO-P_{org} and the SOC content for both data series, i.e. topsoils from tropical and temperate climates. The relationship is described empirically using a single regression model ($R^2 = 0.53$, n = 37). This observation suggests that the difference between AO-P_{tot} and AO-PO_4 is due to the presence of organic P (P_{org}) in the AO-extracts (Jørgensen et al., 2015; Wolf and Baker, 1990).

At a low value of P-total in the AO extracts, the relative contribution of the inorganic PO_4 fraction is generally lower than at higher values of P-total. This is particularly evident for the series of tropical topsoils (Fig. S1).

For our set of weathered tropical topsoils, the fraction of ortho-PO_4 is on average only about 0.55 while for the topsoils from a temperate climate studied previously (Mendez et al., 2020) this contribution is higher (on average 0.74, see Table 2). In combination, Fig. 3a and b suggest that SOM contributes to the extraction of P_{org} in topsoils, and underline the potentially significant contribution of P_{org} to the availability of P and the overall P cycle in weathered tropical topsoils (Nziguheba and Bünemann, 2005; Turner, 2006).

3.3. Reactive metal (hydr)oxides in weathered tropical soils

3.3.1. The reactive surface area

The reactive surface area (RSA) of our sub-Saharan African soils, calculated with Fh as a proxy, varies by a factor of ~20, over the range of ~2–40 m^2 g^{-1} soil (Table 1). In the case of using goethite as reference metal (hydr)oxide, the variation is less and covers the range ~1.5–15 m^2 g^{-1} soil (Table 1). The RSA values calculated with goethite as reference are generally lower than the values obtained by using Fh as reference metal (hydr)oxide. The opposite has been found for the set of P-rich soils from temperate climates analyzed in our previous study (Mendez et al., 2020). The remarkably different behavior of both categories of soils with respect to the calculation of the RSA can be understood from the large difference in the shape of the competitive PO_4 isotherms of goethite and Fh in 0.5 M $NaHCO_3$ at pH 8.5 (Mendez et al., 2020). These isotherms (Fig. S2) relate the concentration of PO_4 (*c*, in μM) in the equilibrium $NaHCO_3$ solution with a corresponding surface PO_4 loading (Γ, in μmol m^{-2}) and are implemented in the CD model to derive the RSA of the soils. The high-affinity character of PO_4 adsorption is much better preserved at relatively low PO_4 concentrations in the case of goethite (Mendez et al., 2020). This leads to a higher PO_4 buffering of the solution by goethite compared to Fh (Mendez et al., 2020; Mendez and Hiemstra, 2019) and consequently, when applied to the soil extracts, this leads to a lower value for the calculated RSA of the soils when goethite is used as reference oxide. As has been discussed previously (Mendez et al., 2020; Mendez and Hiemstra, 2019), at higher PO_4 concentrations, the difference in PO_4 buffer capacity of both Fe (hydr)oxides reverses. At these conditions, the PO_4 buffering is higher for Fh than for goethite (Fig. S2), and consequently, the calculated RSA gets lower for soils when using Fh as proxy. In the temperate soils, the loading of PO_4 is relatively high, while in the tropical soils it is relatively less. This difference results in an opposite outcome of the CD modelling with regard to the derived RSA values (Mendez et al., 2020).

In Section 3.2.1, we have concluded, based on the comparison between R-PO_4 and AO-PO_4, that the interaction between the reactive fraction of the metal (hydr)oxides and PO_4 in our set of tropical topsoils can be best described using Fh as reference metal (hydr)oxide in the CD modelling. The use of the latter metal (hydr)oxide leads to relatively large RSA values in comparison with the use of well-crystallized goethite, as discussed above. However, the question arises whether the fraction of well-crystallized Fe and Al (hydr)oxides also contribute to

Table 2

Comparison of experimental and modelling results for the tropical topsoils from this study and the set of topsoils from a temperate climate studied previously (Mendez et al., 2020). Fe and Al were measured in acid ammonium oxalate (AO) and dithionite-citrate (DC) extractions. P_{tot} and PO_4 were measured in the AO extracts by ICP-OES and the colorimetric molybdenum blue method, respectively. Based on the probe-ion method described by Hiemstra et al.(2010a), the reactive surface area (RSA), reactive PO_4 pool (R-PO_4), and surface loading of PO_4 (Γ_{PO4}) were calculated using Fh as reference metal (hydr)oxide in the CD model calculations (Mendez et al., 2020).

	AO		DC		AO/DC		AO		Probe-ion method		
	Fe	Al	Fe	Al	Fe	Al	PO_4/P_{tot}	$PO_4/(Fe + Al)$	R-PO_4	RSA	Γ_{PO4}
	mmol kg^{-1}				ratio		ratio		mmol kg^{-1}	m^2 g^{-1}	μmol m^{-2}
Weathered tropical topsoils (sub-Saharan African soils)											
Mean	49	101	448	165	0.12	0.59	0.55	0.03	2.8	14.3	0.36
Min	8	24	67	39	0.05	0.38	0.37	0.01	0.9	1.7	0.04
Max	156	314	996	329	0.34	0.96	1.00	0.15	14.3	39.1	1.47
Temperate climate topsoils* (The Netherlands)											
Mean	102	29	188	34	0.58	0.80	0.76	0.13	12.5	9.0	1.64
Min	11	3	16	6	0.28	0.50	0.60	0.03	3.2	2.1	0.51
Max	342	58	852	59	0.95	1.30**	0.91	0.48	27.9	19.5	3.44

* For the soil from the temperate regions, soil extractions with dithionite-citrate-bicarbonate (DCB) solution were performed, rather than the dithionite-citrate (DC) extraction used in the present study. Details of the DCB extraction procedure are described inHiemstra et al.(2010a)

** For one soil sample, the measured Al content in the AO soil extracts was higher than in the DCB extracts.

the soil reactivity toward PO_4. This will be discussed next.

Fig. 4 shows that the calculated RSA of our tropical soils is positively correlated to the amount of Fe and Al, either extracted with AO (spheres) or DC (squares). The slope of the regression lines (dashed lines in Fig. 4) approximates the mean specific surface area (SSA) of the metal (hydr) oxide fraction across the soil samples. It leads to a mean value of SSA = 110 ± 22 m^2 $mmol^{-1}$ when the RSA values are scaled to the content of $[Fe + Al]_{AO}$ and SSA = 23 ± 5 m^2 $mmol^{-1}$ in the case of scaling to the content of $[Fe + Al]_{DC}$. This large difference is due to the significant contribution of well-crystallized Fe and Al (hydr)oxides ($[Fe + Al]_{Cryst}$) to the total Fe and Al measured in the DC soil extracts. For the tropical topsoils, the mean SSA value obtained by scaling the RSA to the $[Fe + Al]_{AO}$ content is about two-fold higher than the mean SSA value found for the agricultural topsoils from a temperate climate, using the probe-ion method (Mendez et al., 2020). As we explain below (Section 3.3.2), the higher surface area per mole of $[Fe + Al]_{AO}$ of the tropical soils may be related to the much larger fraction of Al ions in the AO extracts of these soils (Table 2).

The data in Fig. 4 show a large scattering around the regression lines. This implies that the values of SSA largely vary amongst the different soils. Expressed in terms of the more conventional unit of m^2 per g oxide, the SSA varies between $\sim$400 and 1750 m^2 g^{-1} when the RSA is scaled to the fraction of $[Fe + Al]_{AO}$ (see Section 3.3.2). In SCM studies applied to soil samples, the RSA is commonly estimated based on the amount of Fe and Al extracted with AO and an assumed "standard" values for the SSA, i.e. 600 m^2 g^{-1} and 100 m^2 g^{-1} for the nano-and crystalline fraction of the metal (hydr)oxides, respectively (Bonten et al., 2008; Dijkstra et al., 2004; Groenenberg et al., 2012; Warrinnier et al., 2019). For about half of our samples, the use of the latter approach leads to a strong deviation compared to the presently measured RSA values (Fig. S3). These

deviations can have important implications for SCM modelling of the solid-solution partitioning of ions that specifically bind to the natural metal (hydr)oxides in soils.

The molar ratio $[Fe + Al]_{AO}/[Fe + Al]_{Cryst}$ is on average $\sim$0.4 in our set of tropical soils. In other words, on a mass basis, the crystalline fraction of metal (hydr)oxides dominates. However, in terms of surface reactivity, the situation will be different because of the relatively large difference in SSA. Nanocrystalline (hydr)oxides typically have a $\sim$10 times higher SSA than well-crystallized (hydr)oxides (Hiemstra et al., 2010a). When performing a multiple regression analysis using $[Fe + Al]_{AO}$ and $[Fe + Al]_{Cryst}$ as two independent variables, only $[Fe + Al]_{AO}$ is found to be significant for explaining the modelled values of RSA (R^2 = 0.87, with $p < 0.05$ for $[Fe + Al]_{AO}$ and $p > 0.5$ for $[Fe + Al]_{Cryst}$). The statistical evaluation suggests that despite the large mass fraction of crystalline Fe and Al (hydr)oxides, the presence of nanocrystalline (hydr)oxides is the major factor that determines the reactivity of the metal (hydr)oxides in this set of highly weathered tropical soils.

According to literature, differences in the pedogenic conditions and weathering stages of soils may affect both the composition of the metal (hydr)oxide fraction (Basile-Doelsch et al., 2005; Cornell and Schwertmann, 2003; Mikutta et al., 2009) and the relative distribution of the various P pools (Weihrauch and Opp, 2018; Yang and Post, 2011). To illustrate this, we have summarized for our soils both the results of the selective dissolution extractions and the CD modelling in Table 2 and compared the present results with previous ones, obtained for soils from a temperate climate (Mendez et al., 2020).

The weathered tropical topsoils have, on a molar basis, a larger contribution of crystalline metal (hydr)oxides, which is reflected in the lower average AO/DC ratio of Fe and Al. Remarkably, as shown in Section 3.2, the reactivity of these topsoils can nevertheless be best described by using nanocrystalline Fh as reference metal (hydr)oxide in SCM calculations. In this respect, our tropical topsoils do not differ from the previously studied set of topsoils from a temperate climate. A clear difference between both types of soils is the molar ratio $PO_4/(Fe + Al)$, measured in AO extracts. For the tropical topsoils, this molar ratio is on average only $\sim$0.03, which is substantially lower than the average ratio of $\sim$0.13 found for the temperate climate topsoils (Mendez et al., 2020). The difference is likely due to the difference in origin and history of the PO_4 fertilization since the sum of Fe and Al in AO is similar between the two soil sets. The difference in the PO_4 status between both soil series is also visible in the average PO_4 surface loading (Γ_{PO4}), calculated with the CD model. Expressed in μmol PO_4 m^{-2} and calculated from Γ_{PO4} = R-PO_4/RSA, it is on average $\sim$5 times lower in the weathered topsoil from the tropics than in the well-fertilized topsoils from a temperate climate studied previously.

3.3.2. Size-dependent properties of the reactive metal (hydr)oxides

As mentioned above, the slope of the regression lines in Fig. 4 approximates the mean SSA of the metal (hydr)oxide fraction expressed in m^2 $mmol^{-1}$. For expressing these SSAs in a more conventional unit of m^2 g^{-1} of metal (hydr)oxides, additional information about the molar mass of the oxide (M_{nano} in g mol^{-1} Fe or Al) is required. Subsequently, the SSA can be translated into an equivalent particle diameter (d), using the mass density (ρ_{nano} in g m^{-3}) of the metal (hydr)oxide particles. In these calculations, the values of M_{nano}, and ρ_{nano} are not constant but particle size-dependent, because of the nano-size nature of the reactive metal (hydr)oxide particles. However, these values can be calculated iteratively. The resulting particle diameter is consistently applied to calculate the values of the Stern layer capacitances which change with surface curvature (Hiemstra and Van Riemsdijk, 2009; Mendez and Hiemstra, 2020).

The above-sketched approach for scaling the RSA to the amount Fe and Al extracted with AO (Mendez et al., 2020) has been applied here. In the present approach, the natural metal (hydr)oxide fraction is considered as a solid phase of two constituting endmembers, represented by Fh ($FeO_{1.4}(OH)_{0.2} \cdot nH_2O$) and nano-sized Al hydroxide ($Al(OH)_3 \cdot nH_2O$). In
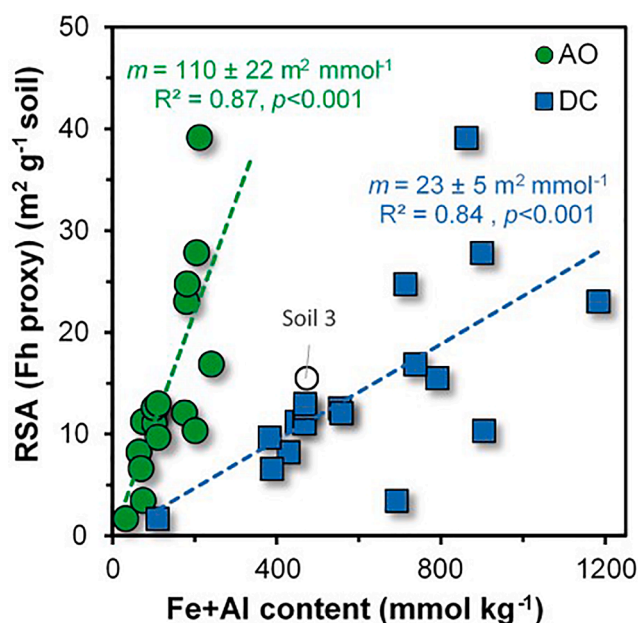
Fig. 4. Relationship between the reactive surface area of soils (RSA), calculated by interpreting the results of the probe-ion method using Fh as reference metal (hydr)oxide in the CD model, and the Fe + Al content measured either in the ammonium oxalate (AO) or in the dithionite-citrate (DC) soil extracts. The dashed lines represent a linear regression analysis where the slopes (m) approximate the mean value of the specific surface area (SSA in m^2 $mmol^{-1}$ Fe + Al) of the natural metal (hydr)oxide fraction. Sample 3 largely deviates from the relationship between $[Fe + Al]_{AO}$ and RSA, which is likely due to an important contribution of Al^{3+} or Al-polymers that can be complexed by SOM in the AO extraction (Jansen et al., 2011) as this sample has a relatively high content of SOM (5%). Therefore, this sample is not considered in the regression analysis of the relationship between $[Fe + Al]_{AO}$ and RSA.

both cases, $n\mathrm{H_2O}$ is the excess amount of chemisorbed water that is due to the presence of surface groups. The overall molar mass of the natural oxide fraction can then be calculated from the weighted sum of the molar masses of the endmembers, according to:

$$M_{\mathrm{soil(hydr)oxide}} = \frac{\mathrm{Fe}}{\mathrm{Fe} + \mathrm{Al}}M_{\mathrm{Fh}} + \frac{\mathrm{Al}}{\mathrm{Fe} + \mathrm{Al}}M_{\mathrm{nanogibbsite}} \quad (1)$$

where Fe and Al are the amounts (mol kg^{-1}) of AO-extractable Fe and Al. In Eq. (1), M_{Fh} and $M_{\mathrm{nanogibbsite}}$ are the molar masses (g mol^{-1} metal ion) of the constituting endmembers Fh and nano Al hydroxide, respectively.

The overall mass density ($\rho_{\mathrm{soil\ (hydr)oxide}}$) can be calculated from the volume-weighted mass densities of both endmembers:

$$\rho_{\mathrm{soil(hydr)oxide}} = \frac{m_1 + m_2}{m_{1/\rho_{\mathrm{nano1}}} + m_{2/\rho_{\mathrm{nano2}}}} \quad (2)$$

in which ρ_{nano1} and ρ_{nano2} are the mass densities (g m^{-3}) and m_1 and m_2 the masses (g kg^{-1}) of the constituting endmembers, i.e. Fh and nano-gibbsite. The latter values (m) follow from the measured metal ion concentrations in the AO extract and the molar masses of both constituting endmembers, i.e. M_{Fh} and $M_{\mathrm{nanogibbsite}}$.

In our approach, the iterative calculations start by considering a spherical metal (hydr)oxide particle with a given diameter (d) for which $M_{\mathrm{soil\ (hydr)oxide}}$ and $\rho_{\mathrm{soil\ (hydr)oxide}}$ are calculated using the values M_{nano} and ρ_{nano} of both nano-endmembers that are derived by applying a set of mathematical relationships given by Hiemstra (2018). Next, the corresponding SSA of the soil metal (hydr)oxide fraction follows from:

$$SSA = \frac{6}{\rho_{\mathrm{soil(hydr)oxide}}d} \quad (3a)$$

and the value obtained can be translated to a corresponding RSA of soil according to:

$$RSA = m_{\mathrm{soil(hydr)oxide}}SSA \quad (3b)$$

in which the mass of the soil metal (hydr)oxide fraction is calculated from the metal ion concentrations measured in the AO extract using as molar masses (M_{nano}) the values of the corresponding metal (hydr)oxide endmembers (Eq. 1). By adapting the mean particle diameter (d), the calculated value of RSA can be brought in line with the experimental value obtained by the probe-ion method. The details of these calculations are described in Mendez et al.(2020), and the final results for each soil are given in Table S1.

Using the above-given set of equations, one can calculate the average particle diameter of the metal (hydr)oxide fraction. Our tropical topsoils have a high contribution of Al to the total Fe + Al content in the AO extracts, on average ~67 ± 8 % on a molar basis, as presented in Table 2. Excluding soil 3, the mean particle diameter of the metal oxides is $d \sim$ 2.3 nm. This particle size is similar to the particle size of Fh freshly prepared in the laboratory (Hiemstra et al., 2019). Such Fh particles have a SSA of $A \sim 700$ m^2 g^{-1}, while we calculate for Al(OH)$_3$·nH$_2$O nanoparticles with the same mean size, a significantly higher SSA of ~1200 m^2 g^{-1}. The reason for the much higher value of SSA is the lower mass density of Al(OH)$_3$·nH$_2$O nanoparticles. In the lattice of the Al hydroxide, the oxygen charge is compensated by light (Al) and very light (H) cations, whereas, in Fh, the dominant cation (Fe) is much heavier, which creates a large difference in mass density (Mendez et al., 2020) and consequently, in SSA between Fe and Al (hydr)oxide nanoparticles of the same diameter (Eq. (3)).

It is essential to acknowledge the differences in the size-dependent values of M_{nano} and ρ_{nano} between the mineral phases of Fe and Al (hydr)oxides, particularly for soils with such high molar Al/Fe ratios as our tropical topsoils. Neglecting these differences, and assuming instead fixed and equal M_{nano} and ρ_{nano} for both representative (hydr)oxide phases, as the Fh core, for instance, would lead to smaller (unrealistic) mean particle sizes and corresponding higher values of SSA (Fig. S4).

For our tropical topsoils, the representative spherical particle size is in the range of 1.4–5.5 nm (Table S2). A similar range has been found for the topsoils from temperate regions studied previously, covering the range of 1.5–5.1 nm (Mendez et al., 2020). At the same size, Al-dominated nanoparticles will contain much fewer metal ions than Fe-dominated nanoparticles (Table S1). If both types of particles are loaded with PO$_4$ at the same surface density (μmol/m^2), the Al-dominated particles will have a much higher PO$_4$ adsorption capacity when the value is expressed per mol metal ion. Such a difference in adsorption capacity has been reported for nanocrystalline Al hydroxide compared to Fh (Liu and Hesterberg, 2011; Tiberg et al., 2020) and the differences in mass density may play an important role in that. So, Al (hydr)oxide dominated soils may have a higher PO$_4$ adsorption capacity at a given mean particle size, compared to soils that are Fe (hydr)oxide dominated.

For our tropical soils, Fh has been used as a proxy in the CD model calculations, whereas the reactive metal (hydr)oxide fraction is Al-dominated. This may influence our results. Adsorption data collected for synthetic materials shows that the adsorption isotherms of PO$_4$ in Fh and Al hydroxide systems have a similar shape (Liu and Hesterberg, 2011; Tiberg et al., 2020). It would suggest a similarity in the PO$_4$ affinity between the two types of materials. If this similarity in affinity and the shape of the isotherm also exists for the PO$_4$ adsorption in 0.5 M NaHCO$_3$ the outcome of our modelling may be rather realistic. The good agreement between R-PO$_4$ and AO-PO$_4$ (Fig. 2a) supports this.

4. Conclusions and implications for future studies

In this contribution, we have presented new insights into the surface reactivity of the metal (hydr)oxides in weathered tropical soils.

In our approach, we use a probe-ion method that is based on measuring the competitive adsorption between PO$_4$ and CO$_3$ in 0.5 M NaHCO$_3$ with a succeeding CD model interpretation. The probe-ion method has been developed and tested previously for P-rich topsoils from temperate climates. Here, we show that this method can also be successfully applied without major methodological adaptations to sub-Saharan African topsoils that are low in P and relatively rich in metal (hydr)oxides. We tested the performance of Fh nanoparticles and well-crystallized goethite as proxies for the reactive metal (hydr)oxide fraction in soils, because for each of these Fe (hydr)oxides consistent intrinsic parameters are available for describing with the CD model the competitive PO$_4$-CO$_3$ interaction in these materials. The surface reactivity of the metal (hydr)oxide fraction of these soils is best explained by using Fh rather than goethite as a proxy oxide material in the CD model calculations. The same conclusion was drawn for agricultural topsoils from a temperate region analyzed in our previous study (Mendez et al., 2020). Considering that the soils from temperate and tropical climates have contrasting chemical and mineralogical properties, this finding is remarkable. The sub-Saharan African soils are relatively rich in crystalline Fe and Al (hydr)oxides while the amount of nanocrystalline metal (hydr)oxide (i.e. Fh-like materials) is relatively small. On a molar basis, only ~25 ± 10% of the metal (hydr)oxide fraction is present as nano-particles in the tropical topsoils, whereas this value is ~60 ± 15% for our topsoils from a temperate climate. Despite the relatively small amount of nano-sized materials, this fraction largely controls the reactivity of the pedogenic metal (hydr)oxides, even if present at low molar concentrations. This is likely due to the up to 10 times larger SSA of nanocrystalline metal (hydr)oxides compared to the fraction of well-crystallized metal (hydr)oxides.

According to our experimental data and modelling results, a significant amount of PO$_4$ does not take part in solid-solution equilibrium reactions. Based on DC soil extractions, on average ~60% of the total PO$_4$ associated with the metal (hydr)oxides is occluded in the crystalline (hydr)oxide fraction. During the AO extraction, a considerable amount of P is released as P$_{\mathrm{org}}$. In our tropical soils, this amount can be as high as ~60% of the total AO extractable P. The contribution of P$_{\mathrm{org}}$ is relatively

high because of the rather low surface loading with inorganic PO_4. For soil systems under intensive and reiterative P fertilization, the relative amount of P_{org} will likely be lower.

Scaling of the RSA to the content of AO-extractable Fe and Al (hydr) oxides reveals a large variation in specific surface area (SSA) of the reactive metal (hydr)oxide fraction. In our tropical soils, the SSA is in the range of ~ 400–$1750 \ m^2 \ g^{-1}$. The corresponding mean particle size is between ~ 1.4 and 5.5 nm and it illustrates that nano-sized particles dominate the reactive fraction of metal (hydr)oxides in the studied set of tropical topsoils.

The nano-sized fraction of metal (hydr)oxides in the studied tropical soils is dominated by Al (hydr)oxide materials. Nevertheless, we found that Fh can be used well as a proxy for describing the surface reactivity of PO_4 in these soils. This success suggests that, within limits, the nano-sized and more reactive fractions of both Fe and Al (hydr)oxides have a similar adsorption behavior. It will be interesting for future research to compare the PO_4 adsorption to Fe and Al (hydr)oxides in the presence of 0.5 M $NaHCO_3$, and to investigate how possible differences can be used to improve the probe-ion method.

Since no parametrized state-of-the-art SCM exists presently for Al $(OH)_3$ nanomaterials, the present approach that effectively uses only Fh as a proxy for the overall reactive metal-(hydr)oxides is justifiable and can strongly improve the applications of state-of-the-art SCM to Al (hydr)oxide rich soils from the tropics. Thus, the present probe-ion method can be considered as a robust approach and is a large improvement compared to traditional methods implemented often in SCM studies that use standard SSA values for the metal (hydr)oxides to quantify the RSA in soils. From a broader perspective, a consistent assessment of the RSA, as outlined in this paper, will enhance the accuracy of SCMs to predict the availability as well as mobility of nutrients and contaminants. This is particularly important for oxyanions (e.g. PO_4^{3-}, AsO_4^{3-}) and heavy metal cations (e.g. Zn^{2+}, Cu^{2+}, Cd^{2+}) with high affinities for binding to the reactive metal (hydr)oxides in soils.

The assessment of the RSA with our probe-ion method, and the subsequent self-consistent analysis of the size-dependent properties of the metal (hydr)oxide nanoparticles, will also contribute to gaining new insights into the interaction mechanisms between the reactive metal (hydr)oxides phases and SOC. These mechanisms are highly relevant from the perspective of soil functioning as a carbon reservoir, as growing evidence suggests that the reactive surfaces of metal (hydr)oxides play a key role in determining the SOC storage capacity of soils in the long term (Basile-Doelsch et al., 2020; Kirsten et al., 2021; Rasmussen et al., 2018), by the formation of chemically stable organo-mineral associations (Kleber et al., 2015). For instance, the probe-ion method can now be implemented to assess the relationships between RSA and SOC content in soil samples with contrasting chemical properties (e.g., pH, amount and speciation of Fe and Al (hydr)oxides, PO_4 and SOC content) due to differences in pedogenic conditions, land use and management, or sample depth.

Declaration of Competing Interest

The authors declare that they have no known competing financial interests or personal relationships that could have appeared to influence the work reported in this paper.

Acknowledgements

Appendix A. Supplementary data

Supplementary data to this article can be found online at https://doi.org/10.1016/j.geoderma.2021.115517.

References

Aguilera, N.H., Jackson, M.L., 1953. Iron oxide removal from soils and clays. Soil Sci. Soc. Am. J. 17 (4), 359–364. https://doi.org/10.2136/sssaj1953.03615995001700040015x.

Barrow, N.J., Shaw, T.C., 1976. Sodium bicarbonate as an extractant for soil phosphate, II. Effect of varying the conditions of extraction on the amount of phosphate initially displaced and on the secondary adsorption. Geoderma 16 (2), 109–123. https://doi.org/10.1016/0016-7061(76)90034-3.

Basile-Doelsch, I., Amundson, R., Stone, W.E.E., Masiello, C.A., Bottero, J.Y., Colin, F., Masin, F., Borschneck, D., Meunier, J.D., 2005. Mineralogical control of organic carbon dynamics in a volcanic ash soil on La Reunion. Eur. J. Soil Sci. 0, 050912034650042. 10.1111/j.1365-2389.2005.00703.x.

Basile-Doelsch, I., Balesdent, J., Pellerin, S., 2020. Reviews and syntheses: the mechanisms underlying carbon storage in soil. Biogeosciences 17, 5223–5242. https://doi.org/10.5194/BG-17-5223-2020.

Bonten, L.T.C., Groenenberg, J.E., Weng, L., van Riemsdijk, W.H., 2008. Use of speciation and complexation models to estimate heavy metal sorption in soils. Geoderma 146 (1-2), 303–310. https://doi.org/10.1016/j.geoderma.2008.06.005.

Borggaard, O.K., 1992. Dissolution of Poorly Crystalline Iron Oxides in Soils by EDTA and Oxalate. Zeitschrift für Pflanzenernährung und Bodenkd. 155 (5), 431–436. https://doi.org/10.1002/jpln.19921550513.

Bortoluzzi, E.C., Pérez, C.A.S., Ardisson, J.D., Tiecher, T., Caner, L., 2015. Occurrence of iron and aluminum sesquioxides and their implications for the P sorption in subtropical soils. Appl. Clay Sci. 104, 196–204. https://doi.org/10.1016/J.CLAY.2014.11.032.

Brunauer, S., Emmett, P.H., Teller, E., 1938. Adsorption of gases in multimolecular layers. J. Am. Chem. Soc. 60 (2), 309–319. https://doi.org/10.1021/ja01269a023.

Chen, C., Thompson, A., 2018. Ferrous iron oxidation under varying pO2 levels: the effect of Fe(III)/Al(III) oxide minerals and organic matter. Environ. Sci. Technol. 52 (2), 597–606. https://doi.org/10.1021/acs.est.7b05102.

Cihacek, L.J., Bremner, J.M., 1979. A simplified ethylene glycol monoethyl ether procedure for assessment of soil surface area1. Soil Sci. Soc. Am. J. 43 (4), 821–822. https://doi.org/10.2136/sssaj1979.03615995004300040045x.

Cornell, R.M., Schwertmann, U., 2003. The Iron Oxides: Structure, Properties, Reactions, Ocurrence and Uses, second ed. WILEY-VCH, Germany.

Coward, E.K., Thompson, A., Plante, A.F., 2018. Contrasting Fe speciation in two humid forest soils: Insight into organomineral associations in redox-active environments. Geochim. Cosmochim. Acta 238, 68–84.

Cui, Y., Weng, L., 2013. Arsenate and phosphate adsorption in relation to oxides composition in soils: LCD modeling. Environ. Sci. Technol. 47 (13), 7269–7276. https://doi.org/10.1021/es400526q.

Di Bonito, M., Lofts, S., Groenenberg, J.E., 2018. In: Environmental Geochemistry: Site Characterization, Data Analysis and Case Histories. Elsevier, pp. 237–305. https://doi.org/10.1016/B978-0-444-63763-5.00012-4.

Dijkstra, J.J., Meeussen, J.C.L., Comans, R.N.J., 2009. Evaluation of a generic multisurface sorption model for inorganic soil contaminants. Environ. Sci. Technol. 43 (16), 6196–6201. https://doi.org/10.1021/es900555g.

Dijkstra, J.J., Meeussen, J.C.L., Comans, R.N.J., 2004. Leaching of heavy metals from contaminated soils: an experimental and modeling study. Environ. Sci. Technol. 38, 4390–4395. https://doi.org/10.1021/es049885v.

Dong, W., Wan, J., 2014. Additive surface complexation modeling of uranium(VI) adsorption onto quartz-sand dominated sediments. Environ. Sci. Technol. 48 (12), 6569–6577. https://doi.org/10.1021/es501782g.

Duffner, A., Weng, L., Hoffland, E., van der Zee, S.E.A.T.M., 2014. Multi-surface modeling to predict free zinc ion concentrations in low-zinc soils. Environ. Sci. Technol. 48 (10), 5700–5708. https://doi.org/10.1021/es500257e.

Dzombak, D.A., Morel, F.F.M.M., 1990. Surface Complexation Modeling: Hydrous Ferric Oxide. John Wiley & Sons.

Eisazadeh, A., Kassim, K.A., Nur, H., 2013. Morphology and BET surface area of phosphoric acid stabilized tropical soils. Eng. Geol. 154, 36–41. https://doi.org/10.1016/j.enggeo.2012.12.011.

Eusterhues, K., Rumpel, C., Kögel-Knabner, I., 2005. Organo-mineral associations in sandy acid forest soils: Importance of specific surface area, iron oxides and micropores. Eur. J. Soil Sci. 56, 753–763. https://doi.org/10.1111/j.1365-2389.2005.00710.x.

Fontes, M.P.F., Weed, S.B., 1996. Phosphate adsorption by clays from Brazilian Oxisols: relationships with specific surface area and mineralogy, Geoderma. Elsevier.

Frossard, E., Sinaj, S., 1997. The isotope exchange kinetic technique: a method to describe the availability of inorganic nutrients. Applications to K, P, S and Zn. Isotopes Environ. Health Stud. 33 (1-2), 61–77. https://doi.org/10.1080/10256019808036360.

Gálvez, N., Barrón, V., Torrent, J., 1999. Effect of phosphate on the crystallization of hematite, goethite, and lepidocrocite from ferrihydrite. Clays Clay Miner. 47, 304–311. https://doi.org/10.1346/CCMN.1999.0470306.

Goldberg, S., 2014. Application of surface complexation models to anion adsorption by natural materials. Environ. Toxicol. Chem. 33 (10), 2172–2180. https://doi.org/10.1002/etc.2566.

Groenenberg, J.E., Dijkstra, J.J., Bonten, L.T.C., De Vries, W., Comans, R.N.J., 2012. Evaluation of the performance and limitations of empirical partition-relations and process based multisurface models to predict trace element solubility in soils. Environ. Pollut. 166, 98–107. https://doi.org/10.1016/j.envpol.2012.03.011.

Groenenberg, J.E., Lofts, S., 2014. The use of assemblage models to describe trace element partitioning, speciation, and fate: a review. Environ. Toxicol. Chem. 33 (10), 2181–2196. https://doi.org/10.1002/etc.2642.

Groenenberg, J.E., Römkens, P.F.A.M., Zomeren, A.V., Rodrigues, S.M., Comans, R.N.J., 2017. Evaluation of the single dilute (0.43 M) nitric acid extraction to determine geochemically reactive elements in soil. Environ. Sci. Technol. 51 (4), 2246–2253. https://doi.org/10.1021/acs.est.6b0515110.1021/acs.est.6b05151.s001.

Guo, H., Barnard, A.S., 2013. Naturally occurring iron oxide nanoparticles: morphology, surface chemistry and environmental stability. J. Mater. Chem. A 1 (1), 27–42. https://doi.org/10.1039/C2TA00523A.

Hass, A., Loeppert, R.H., Messina, M.G., Rogers, T.D., 2011. Determination of phosphate in selective extractions for soil iron oxides by the molybdenum blue method in an automated continuance flow injection system. Commun. Soil Sci. Plant Anal. 42 (14), 1619–1635. https://doi.org/10.1080/00103624.2011.584598.

Heister, K., 2014. The measurement of the specific surface area of soils by gas and polar liquid adsorption methods—limitations and potentials. Geoderma 216, 75–87. https://doi.org/10.1016/j.geoderma.2013.10.015.

Hengl, T., Mendes De Jesus, J., Heuvelink, G.B.M., Gonzalez, M.R., Kilibarda, M., Blagotí, A., Shangguan, W., Wright, M.N., Geng, X., Bauer-Marschallinger, B., Guevara, M.A., Vargas, R., Macmillan, R.A., Batjes, N.H., Leenaars, J.G.B., Ribeiro, E., Wheeler, I., Mantel, S., Kempen, B., 2016. SoilGrids250m: global gridded soil information based on machine learning. PLoS One.

Hiemstra, T., 2018. Ferrihydrite interaction with silicate and competing oxyanions: geometry and hydrogen bonding of surface species. Geochim. Cosmochim. Acta 238, 453–476. https://doi.org/10.1016/j.gca.2018.07.017.

Hiemstra, T., Antelo, J., Rahnemaie, R., Riemsdijk, W.H.V., 2010a. Nanoparticles in natural systems I: the effective reactive surface area of the natural oxide fraction in field samples. Geochim. Cosmochim. Acta 74 (1), 41–58. https://doi.org/10.1016/j.gca.2009.10.018.

Hiemstra, T., Antelo, J., van Rotterdam, A.M.D.(., van Riemsdijk, W.H., 2010b. Nanoparticles in natural systems II: The natural oxide fraction at interaction with natural organic matter and phosphate. Geochim. Cosmochim. Acta 74 (1), 59–69. https://doi.org/10.1016/j.gca.2009.10.019.

Hiemstra, T., Mendez, J.C., Li, J., 2019. Evolution of the reactive surface area of ferrihydrite: time, pH, and temperature dependency of growth by Ostwald ripening. Environ. Sci. Nano 6 (3), 820–833. https://doi.org/10.1039/C8EN01198B.

Hiemstra, T., Van Riemsdijk, W.H., 2009. A surface structural model for ferrihydrite I: sites related to primary charge, molar mass, and mass density. Geochim. Cosmochim. Acta 73 (15), 4423–4436. https://doi.org/10.1016/j.gca.2009.04.032.

Hiemstra, T., Van Riemsdijk, W.H., 1996. A surface structural approach to ion adsorption: the charge distribution (CD) model. J. Colloid Interface Sci. 179 (2), 488–508. https://doi.org/10.1006/jcis.1996.0242.

Hiemstra, T., Zhao, W., 2016. Reactivity of ferrihydrite and ferritin in relation to surface structure, size, and nanoparticle formation studied for phosphate and arsenate. Environ. Sci. Nano 3 (6), 1265–1279. https://doi.org/10.1039/C6EN00061D.

Houba, V.J.G., Temminghoff, E.J.M., Gaikhorst, G.A., van Vark, W., 2000. Soil analysis procedures using 0.01 M calcium chloride as extraction reagent. Commun. Soil Sci. Plant Anal. 31 (9-10), 1299–1396. https://doi.org/10.1080/00103620009370514.

ISO, 2012a. ISO 12782-3:2012 Soil quality – Parameters for geochemical modelling of leaching and speciation of constituents in soils and materials – Part 3: Extraction of aluminium oxides and hydroxides with ammonium oxalate/oxalic acid.

ISO, 2012b. ISO 12782-2:2012 - Soil quality – Parameters for geochemical modelling of leaching and speciation of constituents in soils and materials – Part 2: Extraction of crystalline iron oxides and hydroxides with dithionite.

Jansen, B., Tonneijck, F.H., Verstraten, J.M., 2011. Selective extraction methods for aluminium, iron and organic carbon from montane volcanic ash soils. Pedosphere 21 (5), 549–565. https://doi.org/10.1016/S1002-0160(11)60157-4.

Jørgensen, C., Turner, B.L., Reitzel, K., 2015. Identification of inositol hexakisphosphate binding sites in soils by selective extraction and solution 31P NMR spectroscopy. Geoderma 257–258, 22–28. https://doi.org/10.1016/j.geoderma.2015.03.021.

Kaiser, K., Guggenberger, G., 2000. The role of DOM sorption to mineral surfaces in the preservation of organic matter in soils, in: Organic Geochemistry. Pergamon, pp. 711–725. 10.1016/S0146-6380(00)00046-2.

Keizer, M.G., Van Riemsdijk, W.H., 1995. ECOSAT, a Computer Program for the Calculation of Chemical Speciation and Transport in Soil-Water Systems. Wageningen, the Netherlands, the Netherlands.

Kennedy, M.J., Pevear, D.R., Hill, R.J., 2002. Mineral surface control of organic carbon in black shale. Science (80-.) 295, 657–660. https://doi.org/10.1126/science.1066611.

Kinniburgh, D.G., 1993. FIT User Guide, Technical Report WD/93/23. Keyworth.

Kirsten, M., Mikutta, R., Vogel, C., Thompson, A., Mueller, C.W., Kimaro, D.N., Bergsma, H.L.T., Feger, K.-H., Kalbitz, K., 2021. Iron oxides and aluminous clays selectively control soil carbon storage and stability in the humid tropics. Sci. Rep. 111 11, 1–12. 10.1038/S41598-021-84777-7.

Kleber, M., Eusterhues, K., Keiluweit, M., Mikutta, C., Mikutta, R., Nico, P.S., 2015. Mineral-organic associations: formation, properties, and relevance in soil environments. Adv. Agron. 130, 1–140. https://doi.org/10.1016/bs.agron.2014.10.005.

Kleber, M., Schwendenmann, L., Veldkamp, E., Rößner, J., Jahn, R., 2007. Halloysite versus gibbsite: silicon cycling as a pedogenetic process in two lowland neotropical rain forest soils of La Selva, Costa Rica. Geoderma 138 (1-2), 1–11. https://doi.org/10.1016/j.geoderma.2006.10.004.

Koopmans, G.F., Hiemstra, T., Vaseur, C., Chardon, W.J., Voegelin, A., Groenenberg, J. E., 2020. Use of iron oxide nanoparticles for immobilizing phosphorus in-situ: Increase in soil reactive surface area and effect on soluble phosphorus. Sci. Total Environ. 711, 135220. https://doi.org/10.1016/j.scitotenv.2019.135220.

Koopmans, G.F., Oenema, O., Van Riemsdijk, W.H., 2004. Characterization, desorption, and mining of phosphorus in noncalcareous sandy soils.

Kopittke, P.M., Dalal, R.C., Hoeschen, C., Li, C., Menzies, N.W., Mueller, C.W., 2020. Soil organic matter is stabilized by organo-mineral associations through two key processes: the role of the carbon to nitrogen ratio. Geoderma 357, 113974. https://doi.org/10.1016/j.geoderma.2019.113974.

Liu, Y.-T., Hesterberg, D., 2011. Phosphate bonding on noncrystalline Al/Fe-hydroxide coprecipitates. Environ. Sci. Technol. 45 (15), 6283–6289. https://doi.org/10.1021/es201597j.

Lookman, R., Freese, D., Merckx, R., Vlassak, K., van Riemsdijk, W.H., 1995. Long-term kinetics of phosphate release from soil. Environ. Sci. Technol. 29 (6), 1569–1575. https://doi.org/10.1021/es00006a020.

Mayer, L.M., 1994. Surface area control of organic carbon accumulation in continental shelf sediments. Geochim. Cosmochim. Acta 58 (4), 1271–1284. https://doi.org/10.1016/0016-7037(94)90381-6.

Mehra, O.P., Jackson, M.L., 1958. Iron oxide removal from soils and clays by a dithionite-citrate system buffered with sodium bicarbonate. Clays Clay Miner. 7, 317–327. https://doi.org/10.1346/CCMN.1958.0070122.

Mendez, J.C., Hiemstra, T., 2020. Surface area of ferrihydrite consistently related to primary surface charge, ion pair formation, and specific ion adsorption. Chem. Geol. 532, 119304. https://doi.org/10.1016/j.chemgeo.2019.119304.

Mendez, J.C., Hiemstra, T., 2019. Carbonate adsorption to ferrihydrite: competitive interaction with phosphate for use in soil systems. ACS Earth Sp. Chem. 3 (1), 129–141. https://doi.org/10.1021/acsearthspacechem.8b00160.

Mendez, J.C., Hiemstra, T., Koopmans, G.F., 2020. Assessing the reactive surface area of soils and the association of soil organic carbon with natural oxide nanoparticles using ferrihydrite as proxy. Environ. Sci. Technol. 54 (19), 11990–12000. https://doi.org/10.1021/acs.est.0c0216310.1021/acs.est.0c02163.s001.

Mikutta, R., Schaumann, G.E., Gildemeister, D., Bonneville, S., Kramer, M.G., Chorover, J., Chadwick, O.A., Guggenberger, G., 2009. Biogeochemistry of mineral-organic associations across a long-term mineralogical soil gradient (0.3-4100 kyr), Hawaiian Islands. Geochim. Cosmochim. Acta 73 (7), 2034–2060. https://doi.org/10.1016/j.gca.2008.12.028.

Mödl, C., Wörmann, H., Amelung, W., 2007. Contrasting effects of different types of organic material on surface area and microaggregation of goethite. Geoderma 141 (3-4), 167–173. https://doi.org/10.1016/j.geoderma.2007.05.003.

Murphy, J., Riley, J.P., 1962. A modified single solution method for the determination of phosphate in natural waters. Anal. Chim. Acta 27, 31–36. https://doi.org/10.1016/S0003-2670(00)88444-5.

Nelson, D.W., Sommers, L.E., 1996. Total Carbon, Organic Carbon, and Organic Matter, in: Methods of Soil Analysis Part 3-Chemical Methods. pp. 961–1010. 10.2136/sssabookser5.3.c34.

Nziguheba, G., Bünemann, E.K., 2005. In: Organic phosphorus in the environment. CABI, Wallingford, pp. 243–268. https://doi.org/10.1079/9780851998220.0243.

Perret, D., Gaillard, J.-F., Dominik, J., Atteia, O., 2000. The diversity of natural hydrous iron oxides. Environ. Sci. Technol. 34 (17), 3540–3546. https://doi.org/10.1021/es0000089.

Rahnemaie, R., Hiemstra, T., van Riemsdijk, W.H., 2007. Carbonate adsorption on goethite in competition with phosphate. J. Colloid Interface Sci. 315 (2), 415–425. https://doi.org/10.1016/j.jcis.2007.07.017.

Rasmussen, C., Heckman, K., Wieder, W.R., Keiluweit, M., Lawrence, C.R., Berhe, A.A., Blankinship, J.C., Crow, S.E., Druhan, J.L., Hicks Pries, C.E., Marin-Spiotta, E., Plante, A.F., Schädel, C., Schimel, J.P., Sierra, C.A., Thompson, A., Wagai, R., 2018. Beyond clay: towards an improved set of variables for predicting soil organic matter content. Biogeochemistry 137 (3), 297–306. https://doi.org/10.1007/s10533-018-0424-3.

Regelink, I.C., Weng, L., Lair, G.J., Comans, R.N.J., 2015. Adsorption of phosphate and organic matter on metal (hydr)oxides in arable and forest soil: a mechanistic modelling study. Eur. J. Soil Sci. 66 (5), 867–875. https://doi.org/10.1111/ejss.2015.66.issue-510.1111/ejss.12285.

Schwertmann, U., 1973. Use of oxalate for the Fe extraction from soils. Can. J. Soil Sci. 53, 244–246. https://doi.org/10.4141/cjss73-037.

Schwertmann, U., 1964. Differenzierung der Eisenoxide des Bodens durch Extraktion mit Ammoniumoxalat-Lösung. Zeitschrift für Pflanzenernährung, Düngung.

Schwertmann, U., Schulze, D.G., Murad, E., 1982. Identification of ferrihydrite in soils by dissolution kinetics, differential X-ray diffraction, and mössbauer spectroscopy. Soil Sci. Soc. Am. J. 46 (4), 869–875. https://doi.org/10.2136/sssaj1982.03615995004600040040x.

Tiberg, C., Sjöstedt, C., Eriksson, A.K., Klysubun, W., Gustafsson, J.P., 2020. Phosphate competition with arsenate on poorly crystalline iron and aluminum (hydr)oxide mixtures. Chemosphere 255, 126937. https://doi.org/10.1016/j.chemosphere.2020.126937.

Tiberg, C., Sjöstedt, C., Gustafsson, J.P., 2018. Metal sorption to Spodosol Bs horizons: organic matter complexes predominate. Chemosphere 196, 556–565. https://doi.org/10.1016/J.CHEMOSPHERE.2018.01.004.

Turner, B.L., 2006. Organic phosphorus in Madagascan rice soils. Geoderma 136 (1-2), 279–288. https://doi.org/10.1016/j.geoderma.2006.03.043.

van der Zee, C., Roberts, D.R., Rancourt, D.G., Slomp, C.P., 2003. Nanogoethite is the dominant reactive oxyhydroxide phase in lake and marine sediments. Geology 31 (11), 993. https://doi.org/10.1130/G19924.110.1130/2003146.

Verbeeck, M., Hiemstra, T., Thiry, Y., Smolders, E., 2017. Soil organic matter reduces the sorption of arsenate and phosphate: a soil profile study and geochemical modelling. Eur. J. Soil Sci. 68 (5), 678–688. https://doi.org/10.1111/ejss.12447.

Warrinnier, R., Goossens, T., Amery, F., Vanden Nest, T., Verbeeck, M., Smolders, E., 2019. Investigation on the control of phosphate leaching by sorption and colloidal transport: column studies and multi-surface complexation modelling. Appl. Geochem. 100, 371–379. https://doi.org/10.1016/j.apgeochem.2018.12.012.

Weihrauch, C., Opp, C., 2018. Ecologically relevant phosphorus pools in soils and their dynamics: the story so far. Geoderma 325, 183–194. https://doi.org/10.1016/j.geoderma.2018.02.047.

Weng, L., Temminghoff, E.J.M., Van Riemsdijk, W.H., 2001. Contribution of individual sorbents to the control of heavy metal activity in sandy soil. Environ. Sci. Technol. 35 (22), 4436–4443. https://doi.org/10.1021/es010085j.

Weng, L., Vega, F.A., Van Riemsdijk, W.H., 2011. Competitive and synergistic effects in pH dependent phosphate adsorption in soils: LCD modeling. Environ. Sci. Technol. 45 (19), 8420–8428. https://doi.org/10.1021/es201844d.

Wiesmeier, M., Urbanski, L., Hobley, E., Lang, B., von Lützow, M., Marin-Spiotta, E., van Wesemael, B., Rabot, E., Ließ, M., Garcia-Franco, N., Wollschläger, U., Vogel, H.-J., Kögel-Knabner, I., 2019. Soil organic carbon storage as a key function of soils - A review of drivers and indicators at various scales. Geoderma 333, 149–162. https://doi.org/10.1016/j.geoderma.2018.07.026.

Wiseman, C.L.S.S., Püttmann, W., Puttmann, W., 2005. Soil organic carbon and its sorptive preservation in central Germany. Eur. J. Soil Sci. 56, 65–76. https://doi.org/10.1111/j.1351-0754.2004.00655.x.

Wolf, A.M., Baker, D.E., 1990. Colorimetric method for phosphorus measurement in ammonium oxalate soil extracts. Commun. Soil Sci. Plant Anal. 21 (19-20), 2257–2263. https://doi.org/10.1080/00103629009368378.

Worsfold, P., McKelvie, I., Monbet, P., 2016. Determination of phosphorus in natural waters: a historical review. Anal. Chim. Acta 918, 8–20. https://doi.org/10.1016/j.aca.2016.02.047.

Xu, R.K., Qafoku, N.P., Van Ranst, E., Li, J.Y., Jiang, J., 2016. Adsorption properties of subtropical and tropical variable charge soils: implications from climate change and biochar amendment. Adv. Agron.. 1–58. https://doi.org/10.1016/bs.agron.2015.09.001.

Yang, X., Post, W.M., 2011. Phosphorus transformations as a function of pedogenesis: a synthesis of soil phosphorus data using Hedley fractionation method. Biogeosciences 8 (10), 2907–2916. https://doi.org/10.5194/bg-8-2907-201110.5194/bg-8-2907-2011-supplement.

Zhang, Y.u., Wu, S., Zheng, H., Weng, L., Hu, Y., Ma, H., 2018. Modes of selenium occurrence and LCD modeling of selenite desorption/adsorption in soils around the selenium-rich core, Ziyang County, China. Environ. Sci. Pollut. Res. 25 (15), 14521–14531. https://doi.org/10.1007/s11356-018-1595-0.